Available online at www.sciencedirect.com
SCIENCE DIRECT®
Inorganica Chimica Acta 349 (2003) 30–36
Inorganica Chimica Acta
www.elsevier.com/locate/ica

Palladium(II) complexes of 4-formylantipyrine *N*(3)-substituted thiosemicarbazones: first example of X-ray crystal structure and description of bonding properties

Paras Nath Yadav [a], Mavroudis A. Demertzis [a,*], Dimitra Kovala-Demertzi [a,*], Stavroula Skoulika [a], Douglas X. West [b]

[a] *Department of Chemistry, University of Ioannina, GR-45110 Ioannina, Greece*
[b] *Department of Chemistry 351700, University of Washington, Seattle, WA 98195-1700, USA*

Received 17 August 2002; accepted 7 January 2003

Abstract

Reaction of 4-formylantipyrine with thiosemicarbazide, *N*(3)-methylthiosemicarbazide and *N*(3)-ethylthiosemicarbazide produced the expected thiosemicarbazones, **1**, **2** and **3**. The three thiosemicarbazones were then reacted with K_2PdCl_4 to produce $[Pd(NS)_2]$ complexes, **4**, **5**, and **6**, respectively, with coordination by the imine nitrogen and thiolate sulfur of the anionic thiosemicarbazone moiety. The thiosemicarbazones and their palladium complexes have been characterized by spectral IR, UV–Vis and ^1H, ^{13}C NMR and electrochemical techniques. The crystal structure of **6** has been obtained and found to be highly symmetrical with a trans arrangement of the two bidentate ligands.

Keywords: Antipyrine; Thiosemicarbazone; Palladium; Crystal structure; Spectral study; Electrochemistry

1. Introduction

Antipyrine (2,3-dimethyl-1-phenyl-5-pyrazolone) and its derivatives possess a wide variety of potentially useful biological properties. Antipyrine is a molecule with minimal protein binding, which is rapidly and completely absorbed from the gastrointestinal tract and extensively metabolized by the cytochrome P-450 liver enzymes [1]. Estimates of half-life and systemic clearance of antipyrine have been used for the in vivo assessment of hepatic drug oxidation in different species [2]. Owing to its low pK_a value and its small degree of plasma protein binding, antipyrine is distributed in total body water.

Thiosemicarbazones have demonstrated significant biological activity and new examples are being tested for their antitumor, antimicrobial, and antiviral activity [2–13]. Palladium(II) and platinum(II) complexes of 2-formylpyridine and 2-acetylpyridine *N*(3)-substituted thiosemicarbazones have been studied with regard to their structural and biological properties, and some of them have shown remarkable antitumor activity [11–13]. This work is an extension of previously studied palladium(II) complexes of 2-acetylpyridine TSC with potentially interesting biological activity [11,12]. Here, we report on the palladium(II) complexes of 4-formylantipyrine *N*(4)-substituted thiosemicarbazones. To our knowledge, this is the first report of a structure of a metal complex of a 4-formylantipyrine *N*(3)-substituted thiosemicarbazone.

2. Experimental

Solvents were purified and dried according to standard procedures. Infrared and far-infrared spectra were recorded on a Nicolet 55XC Fourier transform spectrophotometer using KBr pellets (4000–400 cm^{-1}) and nujol mulls dispersed between polyethylene disks (400–40 cm^{-1}). UV spectra were acquired with a JASCO V-

* Corresponding authors. Tel.: +30-6-514 4825.
E-mail address: dkovala@cc.uoi.gr (D. Kovala-Demertzi).

0020-1693/03/$ - see front matter
doi:10.1016/S0020-1693(03)00087-2

570 spectrophotometer UV/VIS/NIR. The ^{1}H (250.13 MHz) and ^{13}C (62.90 MHz) spectra were obtained on a Bruker AMX-400 spectrometer at room temperature with the signal of free DMSO or $CHCl_3$ (at 2.49 and 7.24 ppm, respectively) as reference. The complexes were analyzed for C, H, N and S in a Carlo-Erba EA 1108 at the University of Ioannina. Analyses of palladium and chlorine were performed in our laboratory by gravimetric and potentiometric techniques, respectively.

Electrochemical measurements were made using an Autolab PGSTAT30 potentiostat with a platinum microsphere as working electrode, a platinum wire auxiliary electrode and an Ag/AgCl reference electrode in a three electrode configuration. Ferrocene was added at the end of each experiment and used as an internal standard. All potentials are reported relative to a Ag/AgCl reference electrode and ferrocinium/ferrocene (Fe^{+}/Fc, $E_{1/2} = 0.173$ V in DMF); under the experimental conditions used (scan rate 100 mV s^{-1}). Et_4NClO_4 (0.1 M) was used as supporting electrolyte, the solutions were 1×10^{-3} M in complex, and all experiments were carried out under a dinitrogen atmosphere.

2.1. Preparation of the complexes and ligands

The ligands HFoATP4DH, **1**, HFoATP4Me, **2**, HFoATP4Et, **3**, were prepared according to the method described previously [15]. The yields and melting points are as follows: **1**, 40.5%, m.p. = 219 °C; **2**, 42.5%, m.p. = 216 °C; **3**, 67.7%, m.p. = 212 °C.

[Pd(FoATP4DH)$_2$], **4**, [Pd(FoATP4Me)$_2$], **5**, [Pd(FoATP4Et)$_2$], **6**, were prepared as follows: to a solution of 1.5 mmol K_2PdCl_4 in 10 ml of distilled water was added 3.2 mmol of a thiosemicarbazone (i.e., **1**, **2**, or **3**). The pH of the solution was adjusted to 8.0–9.0 by the addition of aqueous 1.0 M NH_3, and the reaction mixture was stirred for 5 h at room temperature. The resulting orange–red powder was filtered off, washed with cold methanol and ether, dried in vacuo over silica gel, and finally redried at 70 °C in vacuo over P_4O_{10}. Melting points, percentage yields and elemental analyses are as follows: **4**, m.p., 234 °C; yield 95%; %Found: C, 45.7; H, 4.1; N, 20.5; S, 9.4; Pd, 15.6; Cl, 0.0;%Calcd. for $C_{28}H_{35}N_{10}O_2S_2Pd$: C, 45.6; H, 4.2; N, 20.5; S, 9.6; Pd, 15.3; Cl, 0.0%; **5**, m.p., 235 °C; yield 92%; %Found: C, 47.3; H, 5.6; N, 19.7; S, 9.0; Pd, 15.6; Cl, 0.0;%Calcd. for $C_{29}H_{34}N_{10}O_2S_2Pd$: C, 47.2; H, 5.2; N, 19.7; S, 9.1; Pd, 15.6; Cl, 0.0%; **6**, m.p., 230 °C; yield 77%; %Found: C, 48.8; H, 4.9; N, 18.9; S, 8.7; Pd, 14.4; Cl, 0.0;%Calcd. for $C_{30}H_{36}N_{10}O_2Pd$: C, 48.8; H, 5.0; N, 19.0; S, 9.6; Pd, 14.4; Cl, 0.0.

2.2. X-ray crystallography

Slow evaporation of a dilute 1:1 by volume CH_3CN/CH_3OH solution provided an orange prismatic crystal of **6**, which was mounted on a glass fiber and used for data collection. Cell constants and an orientation matrix for data collection were obtained by least-squares refinement of the diffraction data from 25 reflections in the range $2.12 < \theta < 25.00°$ on a Bruker-P4 diffractometer. Data were collected at 293 K using Mo Kα radiation ($\lambda = 0.71073$ Å) and the ω-scan technique, and corrected for Lorentz and polarization effects [19]. A semi-empirical absorption correction (Ψ-scans) was made. The structure was solved by Patterson and Fourier methods [20] and refined on F^2 by a full-matrix least-squares procedure using anisotropic displacement parameters [19]. All hydrogen atoms were located in their calculated positions (C–H 0.93–0.97 Å) and refined using a riding model. Atomic scattering factors are from the 'International Tables for X-ray Crystallography' [19] and molecular graphics from PLATON2001 [20]. A summary of the crystal data, experimental details and refinement results are listed in Table 1.

Table 1
Crystallographic data for the X-ray diffraction studies for [Pd(FoATP4NEt)$_2$]

Empirical formula	$C_{30}H_{36}N_{10}O_2PdS_2$
Formula weight	739.25
Temperature (K)	293(2)
Radiation (Å)	Mo Kα, $\lambda = 0.71073$
Crystal system	Monoclinic
Space group	$P2_1/n$
Unit cell dimensions	
a (Å)	11.0670(10)
b (Å)	14.0970(10)
c (Å)	11.690(3)
β	115.350(10)
V (Å^3)	1648.2(5)
Z	4
D_{calc} (mg m^{-3})	0.427
Absorption coefficient (mm^{-1})	0.316
F(0 0 0)	214
Crystal size (mm)	0.20 × 0.20 × 0.30
θ range for data collection	2.12–25.00
Limiting indices	$0 \leqslant h \leqslant 13$, $-1 \leqslant k \leqslant 14$, $-13 \leqslant l \leqslant 12$
Reflections collected/unique	3230/2817 [$R_{int} = 0.0555$]
Completeness to $\theta = 25.00$	97.10%
Refinement method	Full-matrix least-squares on F^2
Data/restraints/parameters	2817/0/213
Final R indices [$I > 2\sigma(I)$]	$R_1 = 0.0639$, $wR_2 = 0.1074$
R indices (all data)	$R_1 = 0.1404$, $wR_2 = 0.1334$
Goodness-of-fit on F^2	1.009
Largest difference peak and hole (eÅ^{-3})	0.395 and −0.437

Table 2
Main IR absorptions (cm^{-1}) for 4-formylantipyrine $N(4)$-substituted thiosemicarbazones and their palladium(II) complexes

	$\nu_{as,s}$(N3H)	$\nu_{as,s}$(N2H)	ν(C=O)	ν(C=N)	δ(N3H)	δ(N2H)	ν(NN)	ν(C=S)	ν(PdN)	ν(PdS)
1	3431s 3252s	3135mb	1634s	1614m	1541b	1489m	1053m	829s		
2	3371s	3213s	1635s	1606w	1529vb	1529vb	1068s	847w		
3	3356s	3057m	1635s	1603m	1515vb	1515vb	1059s	887s		
4	3444w 3307s		1618s	1589w 1582w	1493b		1082m	740m	432m	342m
5	3382mb		1653s	1619m 1589m	1503b		1085m	773s	448s	356m
6	3356sh 3292b		1648s	1593s	1497b		1083m	766s	397s	357s

3. Results and discussion

3.1. Spectroscopic and electrochemical studies

The IR spectral bands most useful for determining a thiosemicarbazone's mode of coordination are given in Table 2. Decreases in the ν(C=N) energy by 20–35 cm^{-1} on complexation are consistent with coordination of the imine nitrogen, as is the presence of a band at ~ 450–500 cm^{-1}, which is assigned to ν(Pd–N). Coordination of the thiolato sulfur is indicated by a decrease in energy of thioamide IV band, as well as by the presence of a band at 340–380 cm^{-1} that is assignable to ν(Pd–S). As expected, greater energy decreases in the thioamide IV band occur for the anionic form of the ligand owing to the C–S entity formally becoming a single bond. A band in the 1634–1642 cm^{-1} region of the spectra of the **1**, **2**, and **3** is assigned to ν(C=O). This band is shifted to 1648–1654 cm^{-1} in the spectra of **4**, **5**, and **6** which, indicates that coordination of the carbonyl oxygen does not occur. The relatively low energy for ν(C=O) bond in the spectra of 4-formylantipyrine thiosemicarbazones and their complexes is indicative that the carbonyl oxygen is involved in hydrogen bonding, i.e., N–H···O [14–18].

The ^{1}H and ^{13}C NMR assignments for thiosemicarbazones and their palladium(II) complexes in d^6-DMSO are shown in Tables 3a, 3b and 4 is not sufficiently soluble in DMSO to obtain an ^{13}C NMR spectrum. The ^{1}H NMR spectra of **1**, **2**, and **3** indicate that they exist primarily as the Z isomer with respect to the imine bond (i.e., C=N1) in solution based on the appearance of the N(2)**H** resonance at ~13.00 ppm, which is indicative of intramolecular hydrogen bonding. The resonance at 10.70–11.10 ppm in the spectrum of the thiosemicarbazones is also assigned to N(2)**H**, which is hydrogen bonded to the d^6-DMSO solvent; it and the resonance at 7.88–7.92 ppm disappear in the presence of D_2O, confirming the assignment of the latter as N(3)**H** [14–18]. The resonances at 13 and 11 ppm are absent in the spectra of the complexes indicating the loss of N(3)**H** and the presence of the anionic thiosemicarbazone moiety in the complexes. The two signals in the range of 6.89–8.09 ppm are assigned to the formyl hydrogen **H**–C=N. This signal and the signal at 7.88–7.92 ppm (N4**H**) are shifted upfield indicating increased electron density at these sites in the palladium(II) complexes. On coordination of the sulfur and imine nitrogen atoms the electron density would be expected to be lost from the **H**–C=N and N3**H** functions, as has been observed for zinc(II) complexes of 4-formylantipyrine $N(4)$-substituted thiosemicarbazones [15] However, π-back bonding from the palladium(II) to the thiolato and imine functions occurs causing an upfield shift of these resonances. The signals owing to C–C**H**$_3$ and N–C**H**$_3$ groups (i.e., pyrazolone ring) are unshifted in the palladium(II) complexes indicating that the carbonyl oxygen is not involved in coordination in solution. The thiosemicarbazone moiety's thione carbon is found in the $\delta = 175.0$–180.0 ppm range and the imine carbon in

Table 3a
^{1}H NMR spectra of 4-formylantipyrine $N(4)$-substituted thiosemicarbazones and their palladium(II) complexes

Compound	C–CH_3	N–CH_3	C_6H_5	H–C=N	N2H	N3H
1	2.44	3.33	7.30–7.60	7.58, 6.92	11.15, 13.09	7.88, 7.92s
2	2.57s	3.24s	7.31–7.60	7.77	11.16, 13.09	7.92s
3	2.44, 2.56	3.24, 3.51	7.27–7.58	7.76, 6.89	11.14, 13.04	7.92s
4	2.42	3.33	7.30–7.63	7.11		6.75
5	2.57	3.25	7.15–7.56	7.66		8.01s
6	2.56, 2.62	3.25	7.14–7.60	6.89		7.63

Table 3b
^{13}C NMR spectra of 4-formylantipirine $N(5)$-substituted thiosemicarbazones and itspalladium(II) complexes in d_6-DMSO

Compound	C–CH_3	N–CH_3	H–C=N	C=O	C=S
1	9.7	33.7, 33.5	152.0, 151.8	163.1	176.3
2	9.7	30.4, 30.0	152.0, 151.7	163.1, 160.9	177.0, 176.5
3	10.2	34.3, 34.0	152.2, 152.5, 151.7	163.5, 161.3	176.4, 175.9
5	10.5	32.2, 32.1	152.9, 152. 5	163.2	174.5
6	10.6	34.9, 34.2	153.1, 152.4	163.6, 163.4, 161.6	176.5, 170.6

Table 4
Selected bond lengths [Å] and angles [°] for **6**

Pd(1)–N(1a)	2.028(5)
Pd(1)–N(1)	2.028(5)
Pd(1)–S	2.285(2)
Pd(1)–Sa	2.285(2)
S–C(4)	1.761(8)
N(1)–C(3)	1.315(9)
N(1)–N(2)	1.378(8)
N(4)–C(7)	1.361(9)
N(4)–N(5)	1.382(8)
N(4)–C(9)	1.472(9)
N(2)–C(4a) 1	1.316(9)
N(5)–C(1)	1.393(8)
N(5)–C(10)	1.429(9)
C(4)–N(2a)	1.316(9)
C(4)–N(3)	1.323(10)
C(1)–O(1)	1.229(9)
N(3)–C(5)	1.457(10)
N(1a)–Pd(1)–N(1)	180.00(13)
N(1a)–Pd(1)–S	82.42(19)
N(1)–Pd(1)–S	97.58(19)
N(1a)–Pd(1)–Sa	97.58(19)
N(1)–Pd(1)–Sa	82.42(19)
S–Pd(1)–Sa	180.00(13)
C(4)–S–Pd(1)	96.6(3)
C(3)–N(1)–N(2)	114.8(6)
C(3)–N(1)–Pd(1)	121.9(5)
N(2)–N(1)–Pd(1)	123.3(5)
C(7)–N(4)–N(5)	108.3(6)
C(7)–N(4)–C(9)	126.1(7)
N(5)–N(4)–C(9)	117.6(6)
C(4a)–N(2)–N(1)	112.5(6)
N(2a)–C(4)–N(3)	120.5(7)
N(2a)–C(4)–S	124.6(6)
N(3)–C(4)–S	114.9(6)
O(1)–C(1)–N(5)	123.5(8)
O(1)–C(1)–C(2)	130.7(7)
C(4)–N(3)–C(5)	124.3(8)
N(3)–C(5)–C(6)	110.7(7)

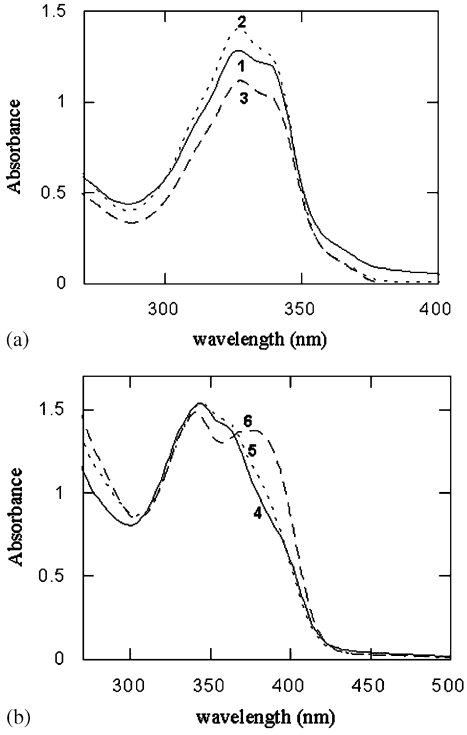

Fig. 1. Electronic absorption spectra of ligands **1–3** (a) and its palladium(II) complexes **4–6** (b) in DMF solution (5×10^{-5} M).

the 152.0 ppm region. The signal at 161.0–163.0 ppm is assigned to the carbonyl carbon, which is in agreement with values found for amide functions [14–18]. In the complexes upfield shifts are observed for **C**=S indicating increased electron density and π-back bonding from palladium(II) to the thiolato carbon. Downfield shifts are observed for CO indicating decreased electron density and may indicate stronger hydrogen bonding in the complexes compared to the ligands.

The bands of **1–3** at ≈310 and 330 nm are due to $\pi \rightarrow \pi^*$ and $n \rightarrow \pi^*$ transitions of the phenyl and pyrazolone rings and the imine portion of the thiosemicarbazone moiety. The energies of these two bands are affected by changes in organic solvents due to differences in the extent and type of hydrogen bonding. The electronic spectra of the ligands and complexes are shown in Fig. 1. The broad band at ≈380–400 cm^{-1} for **4–6** is assignable to Homo–Lumo transition. The Homo orbital is mainly centered on pyrazolone rings and the imine portion of the thiosemicarbazone moieties, while the Lumo orbital is a mixed orbital centered on the metal center and the four donor atoms, d(Pd)/p(S)/p(N). The strong bands at ≈340 cm^{-1} is assignable to intraligand and charge transfer transitions [18,21,22]. The UV spectrum of **6** was computed by

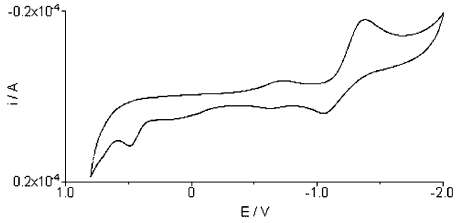

Fig. 2. Cyclic voltammograms (100 mV s^{-1}) of complex **6** in DMF (1.0 mM) in the range +1.0–2.0 V. The quoted potentials are vs ferrocene/ferrocenium.

using single point calculations at the ZINDO/S singly excited interaction configuration level on the molecule **6** [24]. The molecular geometry of **6** was established by using the crystallographic coordinates of the complex.

The cyclic voltammogram of **1**, **2**, and **3** in DMF solution exhibits an irreversible cathodic wave in the negative margin at −1.41, −1.38 and −1.43 V, respectively. This results from the reduction of the imine and thioamide groups present in the thiosemicarbazone moiety, and its value is comparable to that observed for other thiosemicarbazones [23,24]. The cyclic voltammograms of the complexes **4**, **5**, and **6** show irreversible reductions at −1.39, −1.35, −1.38 V, respectively. These values indicate that the reduction process in the complexes is more easily accomplished than the reduction of the free thiosemicarbazones. The electrochemical data suggest that the reduction of **4–6** might be regarded as being more or less centered on the metal center. The electron transfers from the platinum cathode and is directed to the π* Lumo orbital. The Lumo orbital of **6** is a mixed orbital centered on the metal center and the four donor atoms, d(Pd)/p(S)/p(N) [24]. Oxidation waves for **4** and **6** are observed at 0.496 and 0.488 V, respectively, and might be regarded as being more or less centered on the ligand system [23,24]. However, in the range from +1 to −2.52 V additional peaks are observed, Fig. 2.

3.2. Crystal structure of [Pd(FoATP4Et)$_2$]

A perspective view of [Pd(FoATP4Et)$_2$], **6**, with the atomic numbering scheme is shown in Fig. 3. The crystallographic data are summarized in Table 1 and selected bond distances and angles are listed in Table 4. The equivalent, anionic FoATP4Et ligands coordinate in a bidentate manner by the imine nitrogen and thiolato sulfur atoms. The trans-S2 and trans-N2 coordination environment is strictly coplanar in this symmetrical complex with N(1)PdN(1a) and SPdSa angles equal to 180.0°. These two five-member rings exhibit a value of Q(2) = 0.096 Å and of F = 352.78° and the closest pucker descriptor is envelope on Pd. The torsion angle between the two chelated rings PdSC(4)N(2)N(1) and PdSaC(4a)N(2a)N(1a) is 0.0°. The torsion angle between the five-membered chelate ring PdSC(4)N(2)N(1) and the two thiosemicarbazone moieties is 1.59°, while the dihedral angles between the five-membered chelate ring PdSC(4)N(2)N(1) and the pyrazolone and phenyl rings are 37.3 and 69.45°, respectively. The negative charge of the ligand is delocalized over the thiosemicarbazone moiety and the S–C bond distances are consistent with increased single bond character, while the imine C–N distances and both thioamide C–N distances indicate considerable double bond character. This is indicative of the coordinated thiosemicarbazone's greater conjugation and more delocalized electron

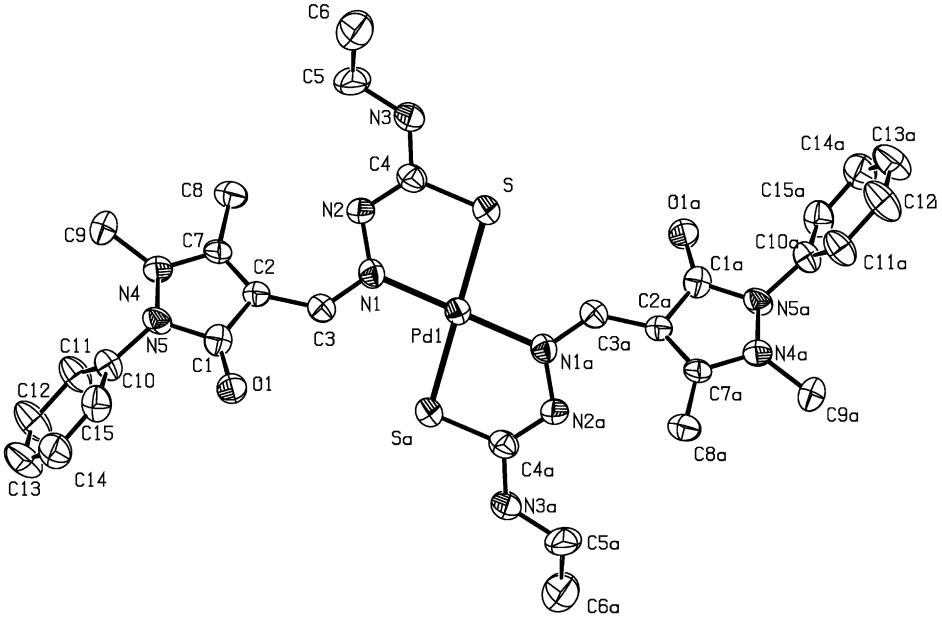

Fig. 3. Perspective view of **6**.

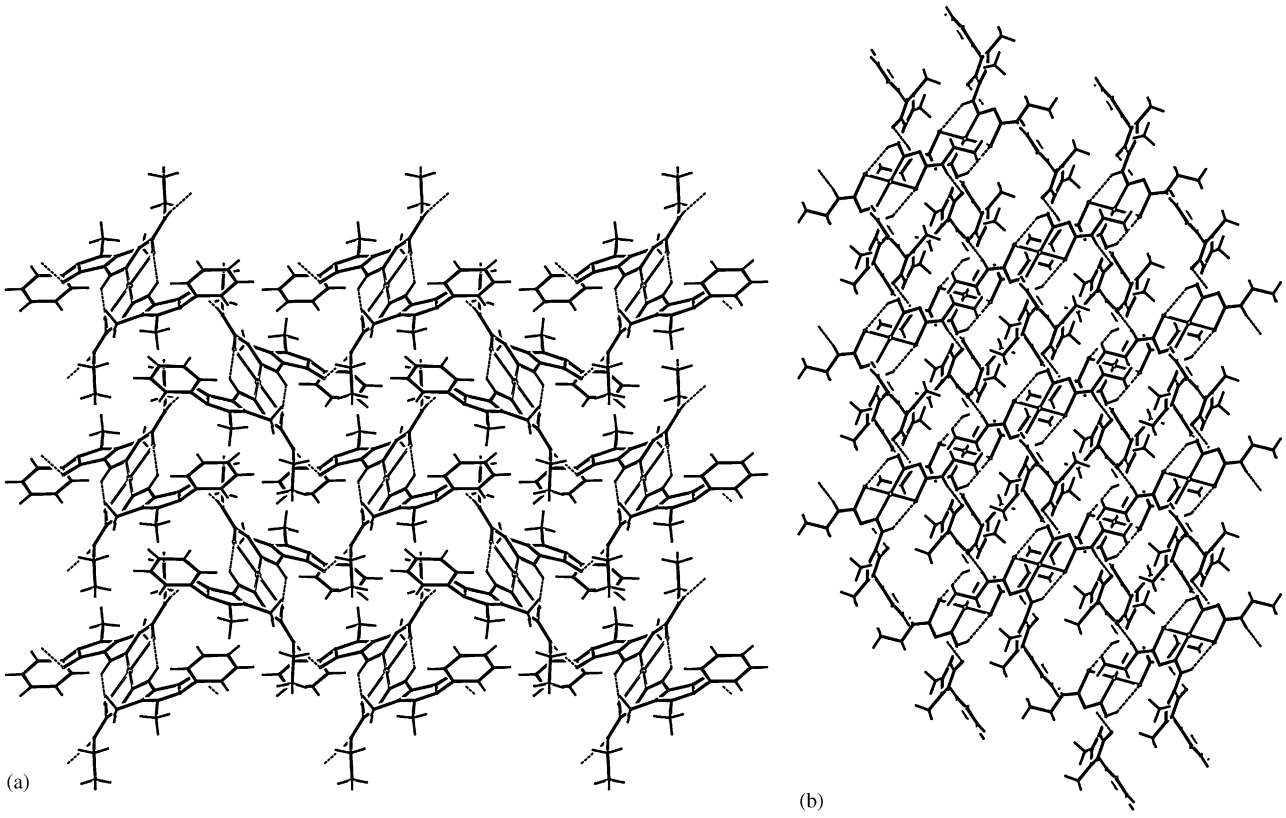

Fig. 4. A view of the extended network of **6** (a) along the *a* axis and (b) along the *b* axis.

density. The Pd–N bond distance, 2.028(7) Å, and Pd–S distance, 2.286(2) Å, are similar to those found in other palladium thiosemicarbazone complexes [22].

The polar hydrogen atom on the thioamide nitrogen participates in an intermolecular hydrogen bond, N–H $\cdots$O, resulting in hydrogen-bonded polymers linked by two of these hydrogen bonds ($1/2-x$, $-1/2+y$, $1/2-z$). These two intermolecular hydrogen bonds connect the monomers, which results in an infinite two-dimensional network. Weak intramolecular hydrogen bonding (i.e., C8–H$\cdots$N4) helps to stabilize the structure, while the crystal packing is determined by strong C–H$\rightarrow\pi$ interactions, Fig. 4.

4. Supplementary material

Crystallographic data i.e., atomic coordinates, thermal parameters, bond lengths and bond angles for **6**, have been deposited with the Cambridge Crystallographic Data Centre CCDC No. 191 088. Copies of this information can be obtained free of charge on application to CCDC, 12 Union Road, Cambridge CB2 1EZ, UK, (fax: +44 1223-336-033 or e-mail: deposit@ccdc.cam.ac.uk.

Acknowledgements

We thank the NMR centrum of the University of Ioannina. PNY thanks IKY for a scholarship. MAD thanks the Research Committee of the University of Ioannina, Project S. Dakaris, for partial funding of this research.

References

[1] H.E. Poulsen, S. Loft, J. Hepatol. 6 (1988) 374.
[2] P.K. Koning, L. Cantilena, Ann. Int. Med. 154 (1994) 590.
[3] A.E. Liberta, D.X. West, Biometals 5 (1992) 121.
[4] I.H. Hall, K.G. Rajendran, D.X. West, A.E. Liberta, Anticancer Drugs 4 (1993) 231.
[5] D.X. West, A.E. Liberta, I.H. Hall, K.G. Rajendran, Anticancer Drugs 4 (1993) 241.
[6] I.H. Hall, S.Y. Chen, K.G. Rajendran, D.X. West, Appl. Organomet. Chem. 10 (1996) 485.
[7] I.H. Hall, M.C. Miller, 3rd, D.X. West, Metal-Based Drugs 4 (1997) 89.
[8] M.C. Miller, 3rd, K.F. Bastow, C.N. Stineman, J.R. Vance, S.C. Song, D.X. West, I.H. Hall, Arch. Pharm. 331 (1998) 121.
[9] M.C. Miller, C.N. Stineman, J.R. Vance, D.X. West, I.H. Hall, Anticancer Res. 18 (1998) 4131.
[10] M.C. Miller, C.N. Stineman, J.R. Vance, D.X. West, I.H. Hall, Appl. Organomet. Chem. 13 (1999) 9.
[11] (a) D. Kovala-Demertzi, P.N. Yadav, M.A. Demertzis, M. Coluccia, J. Inorg. Biochem. 78 (2000) 347;

(b) D. Kovala-Demertzi, M.A. Demertzis, V. Varagi, A. Papageorgiou, D. Mourelatos, E. Mioglou, Z. Iakovidou, A. Kotsis, Chemotherapy 44 (1998) 421;
(c) Z. Iakovidou, E. Mioglou, D. Mourelatos, A. Kotsis, M.A. Demertzis, A. Papagoergiou, J.R. Miller, D. Kovala-Demertzi, Anticancer Drugs 12 (2001) 65.

[12] (a) T. Varadinova, D. Kovala-Demertzi, M. Rupelieva, M. Demertzis, P. Genova, Acta Virologica 45 (2001) 87;
(b) A. Papageorgiou, Z. Iakovidou, D. Mourelatos, E. Mioglou, L. Boutis, A. Kotsis, D. Kovala-Demertzi, A. Domopoulou, D.X. West, M.A. Demertzis, Anticancer Res. 17 (1997) 247;
(c) D. Kovala-Demertzi, A. Domopoulou, M.A. Demertzis, A. Papageorgiou, D.X. West, Polyhedron 16 (1997) 3625.

[13] (a) D. Kovala-Demertzi, M.A. Demertzis, J.R. Miller, C. Papadopoulou, C. Dodorou, G. Filousis, J. Inorg. Biochem. 86 (2001) 555;
(b) D. Kovala-Demertzi, A. Domopoulou, G. Valle, M.A. Demertzis, A. Papageorgiou, J. Inorg. Biochem. 68 (1997) 147.

[14] A.K. El-Sawaf, D.X. West, F.A. El-Saied, R.M. El-Bahnasawy, Synth. React. Inorg. Met-org. Chem. 27 (1997) 1127.

[15] A.K. El-Sawaf, D.X. West, F.A. El-Saied, R.M. El-Bahnasawy, Trans. Met. Chem. 22 (1997) 360.

[16] A.K. El-Sawaf, D.X. West, R.M. El-Bahnasawy, F.A. El-Saied, Trans. Met. Chem. 23 (1998) 227.

[17] A.K. El-Sawaf, D.X. West, F.A. El-Saied, R.M. El-Bahnasawy, Trans. Met. Chem. 23 (1998) 417.

[18] A.K. El-Sawaf, D.X. West, F.A. El-Saied, R.M. El-Bahnasawy, Trans. Met. Chem. 23 (1998) 649.

[19] (a) G.M. Sheldrick, Acta Crystallogr. A 46 (1990) 467;
(b) G.M. Sheldrick, SHELXL-97. Program for the Refinement of Crystal Structures, University of Göttingen, Göttingen, Germany, 1997.

[20] E.A.L. Spek, PLATON, 'A Multipurpose Crystallographic Tool, Utrecht University, Utrecht, The Netherlands, 2001.

[21] A.B.P. Lever, Inorganic Electronic Spectroscopy, Elsevier, New York, 1984.

[22] (a) D. Kovala-Demertzi, N. Kourkoumelis, D.X. West, J. Valdés-Martínez, S. Hernández-Ortega, Eur. J. Inorg. Chem. (1998) 861;
(b) D. Kovala-Demertzi, N. Kourkoumelis, M.A. Demertzis, J.R. Miller, C.S. Frampton, J.K. Swearingen, D.X. West, Eur. J. Inorg. Chem. (2000) 727.

[23] (a) D. Kovala-Demertzi, A. Domopoulou, M.A. Demertzis, J. Valdés-Martínez, S. Hernández-Ortega, G. Espinosa-Pérez, D.X. West, M.M. Salberg, G.A. Bain, P.D. Bloom, Polyhedron 15 (1996) 2587;
(b) D. Kovala-Demertzi, A. Domopoulou, M.A. Demertzis, A. Papageorgiou, D.X. West, Polyhedron 16 (1997) 3625.

[24] HYPERCHEM, Release 6.01 for windows, Molecular Modeling System, Hypercube, Inc., Gainsville, FL, 2000.